Digest Journal of Nanomaterials and Biostructures Vol. 17, No. 4, October-December 2022, p. 1151-1161

Effects of controlled shot peening on multi-scale morphology and hydrophobicity of 316L stainless steel

J. Y. Zhang, L. J. Qin, F. G. Liu, C. S. Lou*
School of Materials Science and Engineering, Shenyang Ligong University, Shenyang 110159, China

In this study, we used shot peening-etching method to construct the multi-scale morphology on the surface of 316L stainless steel, assisted by surface modification to improve hydrophobicity. The effects of the diameter of projectile (0.2, 0.3, 0.4 mm) and shot peening time (1, 1.5, 2, 2.5 min) on the multi-scale morphology and hydrophobicity of the samples were studied. Meanwhile, the surface morphology was examined by metallographic microscope (OM) and scanning electron microscope (SEM). The surface profile and roughness were characterized by laser scanning confocal microscope (LSCM). The fractal dimension D was calculated by data analysis software, and the static contact angle measuring instrument was used to evaluate the hydrophobic performance. The results show that the smaller the diameter of projectile is, the stronger the hydrophobicity of the sample is, and there is the best time for shot peening. Moreover, the size and distance of pits on the surface decrease as the diameter of projectile decreases. The roughness of the surface shows a tendency to increase first and decrease with the increase of shot peening time, and the contact angle has the same tendency. The contact angle of the sample surface increases as the fractal dimension D increases. When the diameter of the projectile is 0.2 mm and the shot peening time is 2 min, after etching and surface modification, the static contact angle is 137.4° and the solid-liquid contact area is only 15.4%. This method has the advantages of low cost, high efficiency and environment-friendly, which is beneficial to the large-scale production of hydrophobic materials.

(Received May 20, 2022; Accepted October 10, 2022)

Keywords: 316L stainless steel, Shot peening, Electrochemical etching, Multi-scale morphology, Hydrophobic performance

1. Introduction

316L stainless steel is widely used in medical and marine fields due to its excellent corrosion resistance, biocompatibility, and high mechanical strength. It plays an indispensable role in offshore oil and gas development engineering. However, the temperature, chloride, surface sewage adhesion, and other factors in the marine environment will cause local corrosion of 316L stainless steel, and it is easy to freeze in winter, affecting the operation of the equipment.

* Corresponding author: chsh_lou@163.com
https://doi.org/10.15251/DJNB.2022.174.1151

Additionally, 316L stainless steel is a commonly used human implant. Its surface bioadhesion makes it easy to absorb non-specific proteins and leads to failure [1]. Therefore, the preparation of hydrophobic 316L stainless steel with self-cleaning and anti-frost properties is of great significance for biomedical and marine anticorrosion. The hydrophobicity of the material surface is determined by the micro-morphology and chemical composition of the surface [2-3].

Generally, there are two ways to prepare hydrophobic surfaces: to construct micro-nano structures on low surface energy materials or to modify low surface energy materials on surfaces with micro-nano structures [4-6]. At present, there are many methods to make the surface of stainless steel hydrophobic, such as laser texture [7-8], electrochemical etching [9-10], chemical etching [11-12], and so on. Yao et al. used nanosecond laser technology to fabricate microstructures of different scales on the surface of 316L stainless steel, and the superhydrophobic material with static contact angle of 160°±5° and dynamic contact angle of 3°±0.5° was obtained [13]. Khaleghi et al. prepared Al_2O_3-13%TiO_2 coating on the surface of AISI 316L stainless steel by a plasma spraying process. Then polytetrafluoroethylene (PTFE) is coated on the prepared coating, and the water contact angle on the surface of the PTFE-modified Al_2O_3-13% TiO_2 coating was 155° [14]. Liu et al. prepared layered Cu-Ni coating on 316L stainless steel by electrodeposition, and then myristic acid was used to reduce the surface energy, and hydrophobic surfaces with water contact angle and slip angle of 161.27° and 7.8° were obtained [15]. However, these methods involve tedious chemical preparation, multiple processing steps, and expensive equipment, which will limit the manufacturing efficiency of hydrophobic products. Compared with other methods of preparing the hydrophobic surface, the shot peening-etching method has the advantages of simple equipment, low cost, and short production cycle, so it is suitable for large-scale production in factories.

In this work, micron pits were prepared by shot peening bombardment of 316L stainless steel. Then the surface of the sample was etched by electrochemical etching to form a multi-scale micro-morphology with a combination of micron and nanometer. Finally, PTFE was used to modify the surface to reduce the surface energy. The material can achieve the double conditions of the hydrophobic property, and its hydrophobic property was studied.

2. Experiment section

2.1. Sample material

The substrate of this experiment is 316L stainless steel (00Cr17Ni14Mo2; Chemical composition: C 0.03% Si 1.00% Mn 2.00% P 0.035% S 0.03% Ni 12.5% Cr 17.5% Mo 2.5%), it was cut in pieces of 30 mm×20 mm×5 mm. The samples were ground on one side with water sandpaper until there was no obvious scratch. Afterward, they were polished with diamond polishing paste, ultrasonically cleaned to remove oil from the surface, and dried for standby.

2.2. Sample preparation

The shot blasting experiment was performed with a combination of a shot blasting machine and air compressor equipment. The diameter of projectile and shot peening time are set as variables respectively. The projectile is made of cast steel. To investigate the effect of shot peening with different diameters on the surface morphology and hydrophobicity, 2 min was bombarded with projectile with diameters of 0.2 mm, 0.3 mm, and 0.4 mm, respectively. To evaluate the effect of shot peening time on the surface morphology and hydrophobicity, the samples were shot peened at 1 min, 1.5 min, 2 min and 2.5 min using a projectile with a diameter of 0.2 mm at a pressure of 0.8 MPa. Subsequently, the treated samples were placed in anhydrous ethanol and sonicated for 10 min, blown dry for standby. The samples after shot peening were placed in 3.5 wt% NaCl solution, and the 316L stainless steel samples were etched by electrochemical etching using the three electrode system of platinum counter electrode, $HgCl_2$ reference electrode and working electrode. Then the samples were completely immersed in 60% PTFE dispersion for 24 hours by atmospheric pressure immersion method and then dried in an oven at 80℃ so that they could not flow. Afterward, they were evaporated and put into a high-temperature furnace and sintered at 350°C (327°C above the melting point of PTFE) for 10 min to form a low surface energy film on the surface of the sample.

2.3. Sample characterization

The surface morphology of the samples was observed by a metallographic microscope (OM; OLYMPUSGX53) and a scanning electron microscope (SEM; Hitachi S-3400N). The surface profile of the samples was characterized by a laser scanning confocal microscope (LSCM; OLS4100), and the surface roughness was also measured by it. Three areas are randomly selected on the sample surface to measure the roughness, and finally take the average. The static contact angle (CA) of the sample surface was measured using a static contact angle measuring instrument (HARKE-SPCA) to characterize its hydrophobic properties. In order to make the measurement results more accurate, the static contact angles were averaged values by measuring at least three different points on each sample surface with a deionized water drop of 5 μl. By using the image processing and numerical calculation function of MATLAB, the corresponding conversion function was compiled, the irregular surface topography with fractal feature was imported, and its information was extracted and analyzed. The program automatically converted the surface topography into grayscale image, then binarized the image, extracted the image boundary through edge detection, and converted the binary image into digital data file. The least square method was used for linear fitting in the double logarithmic coordinates of the data points, and the fractal dimension D of the surface topography was obtained.

3. Results and discussion

3.1. Surface morphology evolution induced by shot peening

Figure 1 displays the microscopic surface morphology of the samples blasted for 2 min with different projectile diameters. As it is clear from Fig.1, there are many pits on the surface of the sample after shot peening. When the shot diameter is 0.2 mm, the pits on the surface of the sample are evident and deep, and the surface undulation is dramatic. The average size of the pits is about 50 μm, and the spacing is 50-100 μm. When the diameter of the projectile is 0.4 mm, the depth of the pits is shallow, the definition is low, the average size of the pits is more than 100μm, and the spacing is more than 100 μm. When the projectiles are driven by high-pressure gas, a high-speed jet is sprayed on the surface of the stainless steel sample, and the original smooth stainless steel surface becomes uneven. The projectile with a small diameter has a small mass.

When the shot peening pressure is the same, the speed of the shot with a small mass is larger, resulting in deep pits and small size. As the diameter of the cast steel shot decreases, the size of the craters on the surface of the sample becomes smaller, and the distribution becomes denser.

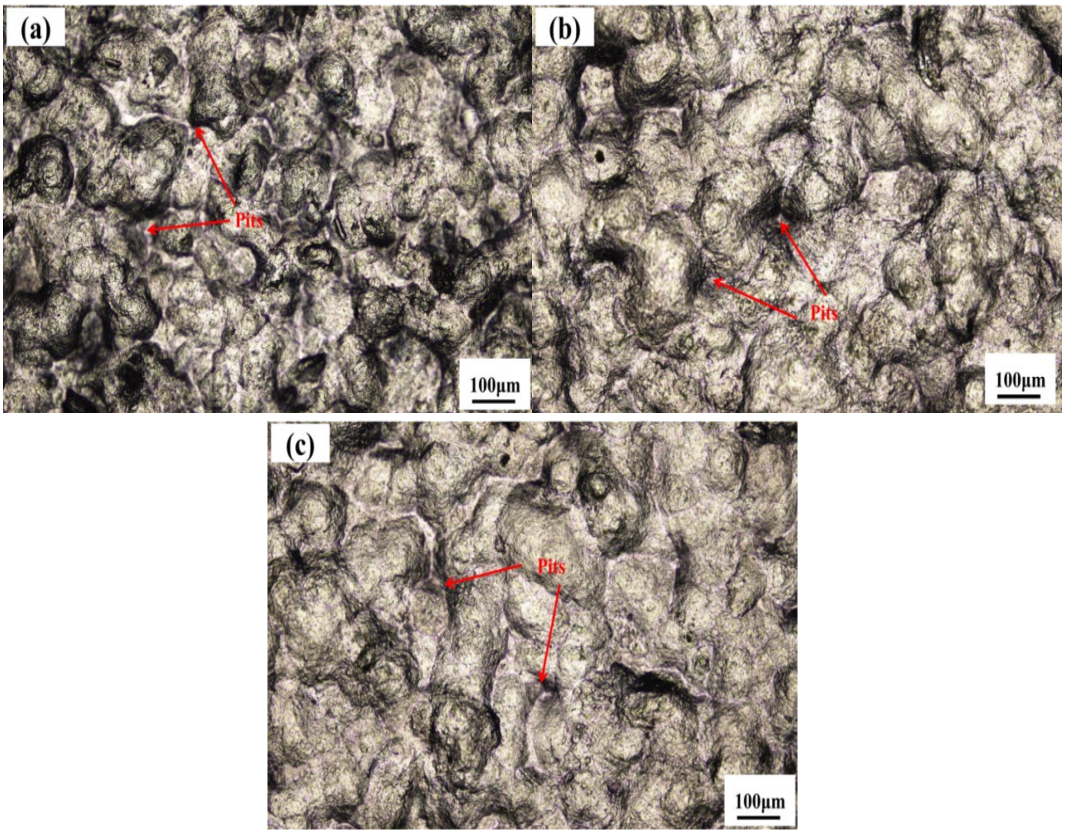

Fig. 1.Microscopic morphology of the sample surface after 2 min for a projectile shot blasting of different sizes: (a)0.2 mm(b)0.3 mm(c)0.4 mm.

Measuring the contact angle is a simple and common method to evaluate wettability. Fig.2 presents the contact angle of the sample surface under different projectile diameters. As shown in Fig.2, the contact angle of the sample surface is 45° without treatment. When the projectile diameter is 0.2 mm, 0.3 mm, and 0.4 mm, the average contact angle is 111°, 98.7° and 96.4°, respectively. This result indicates that the decrease in projectile diameter leads to a decrease in pit size and distance, which leads to an increase in contact angle. Our results are similar to those of Khalili [16-17] et al.

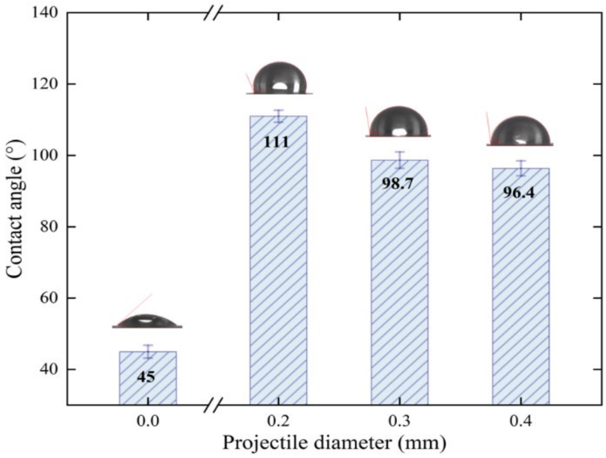

Fig. 2. The relationship between projectile size and contact angle.

3.2. Micro-morphology of shot peening-etched 316L samples

The samples were blasted with 0.2 mm diameter projectile for 1 min, 1.5 min, 2 min, and 2.5 min, respectively, followed by electrochemical etching. SEM images of the surface morphology of the samples are shown in Fig.3.

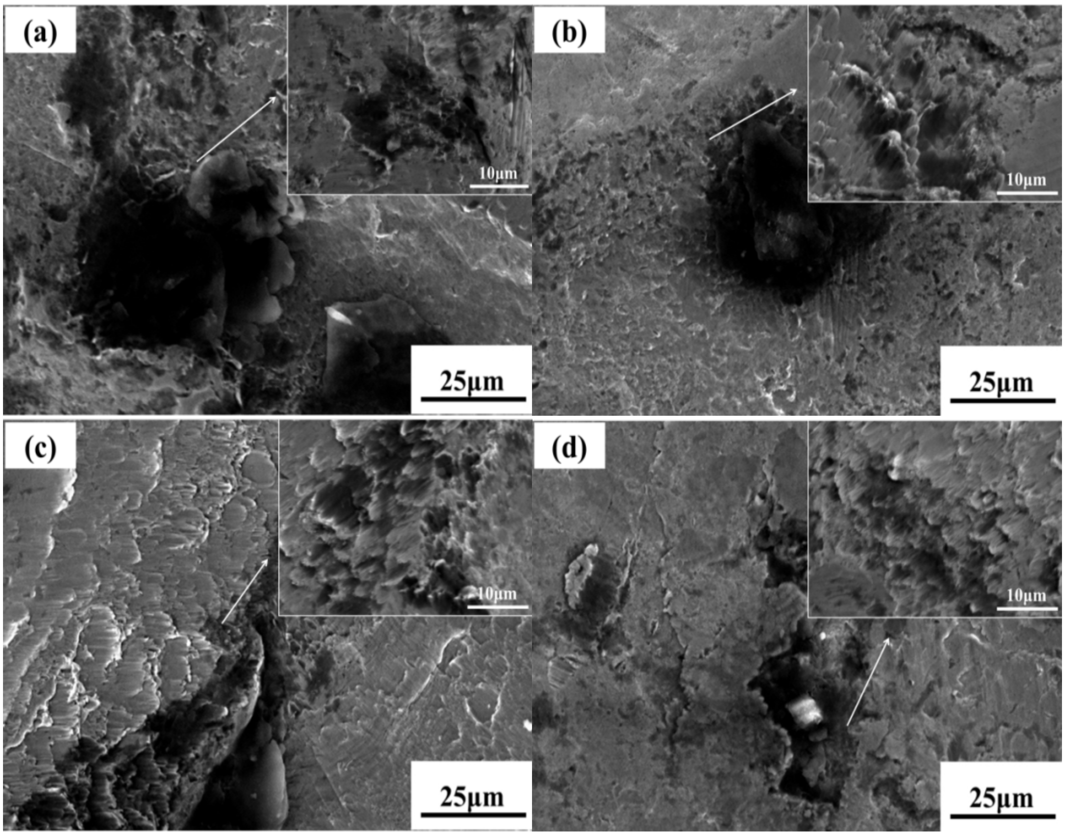

Fig. 3. SEM images of the samples shot peened and electrochemical etched for(a)1 min (b)1.5 min (c)2 min (d)2.5 min.

It can be seen that the surface complexity of the samples after shot peening-etching increases, forming micron-sized pits and numerous microstructures appearing at the edges of them. We magnified these microstructures and found some nanoscale protuberances. A possible explanation for this might be that high speed shot peening causes strong plastic deformation of the surface structure of the sample, resulting in a continuous residual stress distribution area. The number of defects, such as grain boundaries and dislocations, increases with increasing shot peening time. When the etching solution is immersed into the substrate, the defects with higher energy are preferentially etched [18, 19], while the substrate around the defects is etched slowly, thus forming sharp protuberances with diameters ranging from hundreds of nanometers to several microns. These protuberances together with micron pits constitute the multi-scale topography.

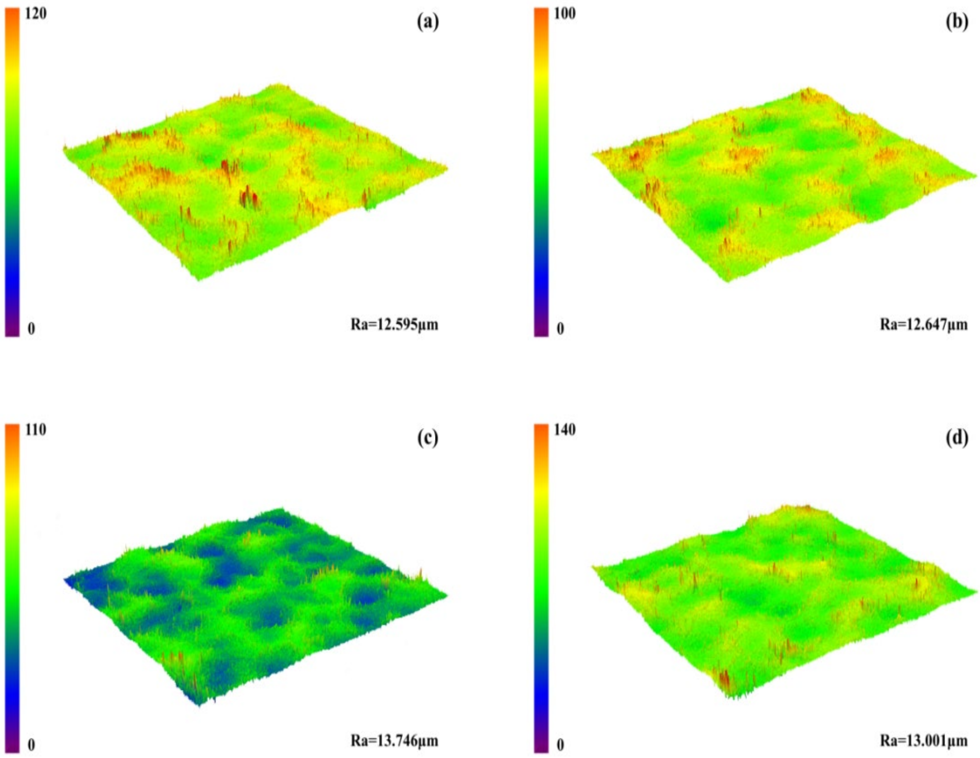

Fig. 4. LSCM images of samples shot peened and electrochemical etched: (a)1 min (b)1.5 min (c)2 min (d)2.5 min.

Fig. 4 demonstrates the LSCM images of the sample surface after shot peening-etching. The change in color in the figure indicates the height change of the pit on the sample surface and its surrounding structure, and the average surface roughness Ra of the sample surface is measured by the laser scanning confocal microscope yet. As can be seen from the figure, when the shot peening time is 1min, there are many original platforms on the surface, and the distribution of pits is uneven. When the shot peening time increases to 2 min, the distribution of pits on the surface is dense and uniform, the pits formed by shot peening appear more microstructure after etching, and the sharp protuberance of the surface increases. With the increase in shot peening time, the surface roughness Ra increases initially and then decreases. This trend could be attributed to the fact that with extension of shot peening time, the surface of the sample is hammered by projectiles, and the coverage of projectiles increases, showing a uniform and dense distribution of pits. For longer shot peening times, the degree of crystal fragmentation on the surface is too large, and the number of defects formed increases. The defects will be etched preferentially because of high energy. After the same etching time, the surface roughness is over etched, exposing the substrate [20], thus showing a decrease in roughness. Initial observations suggest that there may be an optimal shot peening time for stainless steel samples, and if the shot peening time is too long, the surface roughness of the samples decreases.

3.3. Hydrophobicity of shot peening-etched 316L samples

The relationship between the contact angle of the sample after shot peening and shot peening time is shown in Fig.5. As can be seen from the figure, the surface contact angle of the sample increases at first and then decreases with the increase of shot peening time, and reaches the maximum value of 125.1° at 1.5 min. Many microstructures are formed by electrochemical etching of the sample on the basis of shot peening. According to the literature [21], this synergistic mechanism increases the surface roughness of the sample. However, with the increase in the diameter and depth of the microstructure, the droplets are easy to fill, which shows that the contact angle decreases [17]. Compared with shot peening alone, the hydrophobicity of the surface after shot peening etching is improved to some extent. Therefore, we have reason to believe that the synergistic effect of micro-nano multi-scale morphology is a critical factor to improve the surface hydrophobicity of 316L stainless steel. For the substrate with the same surface energy, the greater the roughness is, the stronger the surface hydrophobicity is. The results are consistent with those of Balordi [22-23] and others.

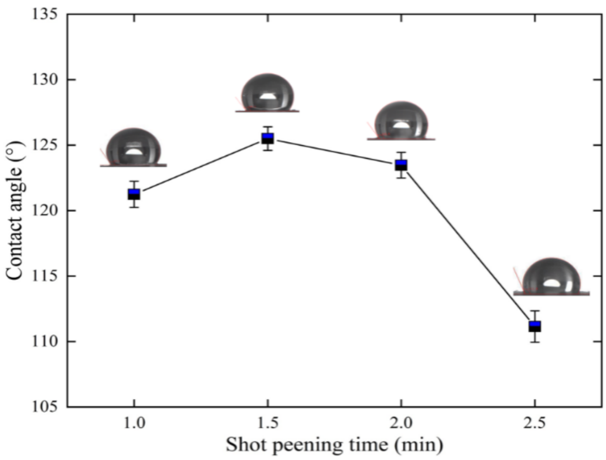

Fig.5.The change curve of static contact angle with time after shot peening-etching.

Fractal dimension is the most important index to evaluate the complexity and irregularity of fractals, and it is feasible to use fractal dimension to characterize micro-morphology [24-25]. The fractal dimension D of the surface after shot peening and shot peening-etching is calculated by MATLAB. The relationship between the fractal dimension D and the contact angle is shown in figure 6. It can be seen that the surface contact angle of the samples after shot peening or shot peening etching increases with the increase of fractal dimension D. This is because the contact angle of the material surface is related to the surface fractal dimension D. The greater the fractal dimension D is, the greater the fluctuation of the sample surface is, which also means that the smaller the percentage of the contact area between the water droplets and the sample surface is, the larger the contact angle is [26-27]. Overall, these results indicate that the wettability of the material surface can be regulated by the fractal dimension D.

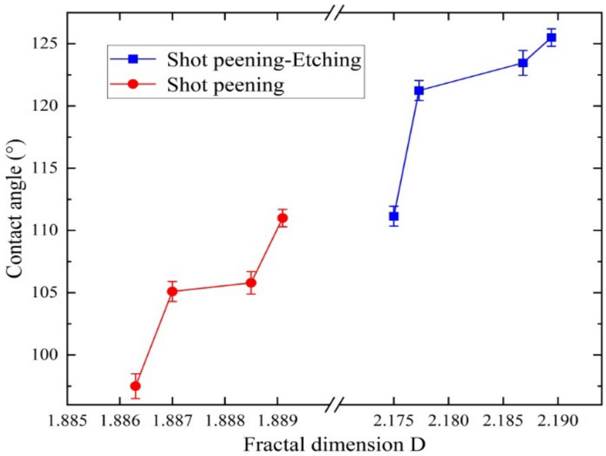

Fig. 6. The relationship between the contact angle and the fractal dimension D under different treatment methods.

3.4. Hydrophobicity of 316L samples after shot peening-etching-surface modification

The surface of 316L stainless steel after shot peening-etching was modified by PTFE. The relationship between the surface static contact angle and shot peening time is shown in Fig.7.

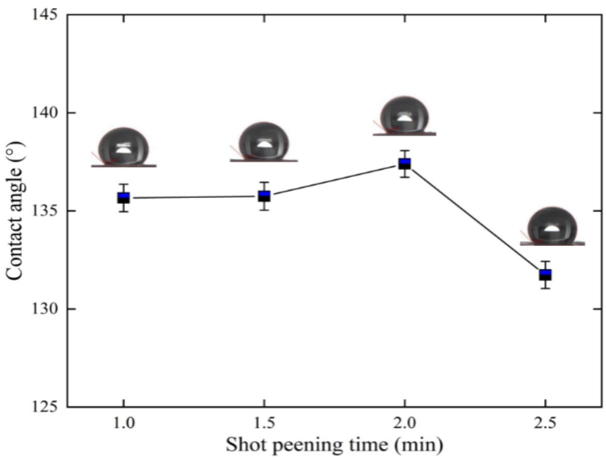

Fig. 7. The change curve of static contact angle with time after shot peening-etching-surface modification.

When the diameter of the projectile is 0.2 mm and the shot peening time is 2 min, the average contact angle after surface modification is 137.4°, which is about 10° higher than that after shot peening and etching. A possible explanation for this might be that the multi-scale rough morphology got by shot peening-etching lays a structural foundation for obtaining hydrophobic properties, and the surface modification changes the chemical composition of the sample surface and reduces the surface tension, thus increasing the contact angle of the sample surface. This synergism is the decisive factor in preparing hydrophobic surfaces [28-29].

According to the Cassie equation, there are bubbles in the grooves between the droplets and the rough surface, which make the droplets unable to fill the grooves on the rough surface. Therefore, increasing the proportion of bubbles will improve the hydrophobicity of the solid surface, according to Cassie equation:

$$\cos\theta_c = f_s(\cos\theta_e + 1) - 1 \tag{1}$$

In the formula, f_s is the ratio of the solid area to the total contact area ($f_s < 1$), θ_c is the apparent contact angle, and θ_e is the intrinsic contact angle. The surface θ_e of 316L stainless steel is 45°. The water contact angle obtained under various treatment conditions is substituted into (1), and the corresponding area fraction of the solid-liquid interface is calculated, as shown in Table 1. The evidence shows that the area fraction of the solid-liquid contact area on the sample surface decreases with the increase of the contact angle. When the diameter of the projectile is 0.2 mm and the shot peening time is 2 min, the surface hydrophobicity is the best when the rough surface is etched and modified with low surface energy. The contact area water droplets and stainless steel surface accounts for only 15.4% of the whole surface. After shot peening and electrochemical etching, the surface of 316L stainless steel forms a multi-scale morphology of micron pits and nanometer protuberances, which can greatly improve the contact angle of the substrate surface [30-32]. It is almost certain that part of the air is trapped in the gap of the morphology, and the size of the water droplet is much larger than that of the micro-topography. When the water drops on the surface, the liquid cannot fill the gap to form a complete solid-liquid contact interface. Instead, it falls on the composite surface composed of micro-nano multi-scale morphology and air, forming a solid-liquid-gas three-phase contact interface. This structure effectively reduces the solid-liquid contact area [33] and makes the surface of 316L stainless steel hydrophobic.

Table 1. Area fraction of solid-liquid interface on sample surface.

Sample（size 0.2 mm , shot peening time 2 min）	CA(°)	f_s(%)
Shot peening	111	37.5
Shot peening - Etching	125.1	24.9
Shot peening - Etching - Surface modification	137.4	15.4

4. Conclusions

In this paper, multi-scale morphologies were prepared on the surface of 316L stainless steel by shot peening-etching method, which laid a foundation for obtaining hydrophobic surface. The effects of projectile diameter and shot peening time on the surface morphology and hydrophobicity of the samples were analyzed. The results show that the smaller the diameter of the projectile is, the stronger the hydrophobicity of the sample is, and there is an optimal shot peening time. When the diameter of the projectile is 0.2 mm and the shot peening time is 2 min, the hydrophobic surface with a contact angle of 137.4° can be obtained after etching and surface modification.

The greater the roughness is, the better the hydrophobicity is. In addition, the study also shows that the fractal dimension D can be used to control the hydrophobic properties of materials. The instruments and equipment used in this experiment have the advantages of low price, short treatment cycle and no release of harmful substances in the treatment process. Therefore, this method is expected to realize the large-scale production of hydrophobic materials.

Acknowledgements

We gratefully acknowledge the Natural Science Foundation of Liaoning Province (2015020228)

References

[1] B. Wu, M. Zhou, J. Li, X. Ye, G. Li, L. Cai, Applied Surface Science**256**(1), 61 (2009);https://doi.org/10.1016/j.apsusc.2009.07.061
[2]S. S. Latthe, C. Terashima, K. Nakata, et al, Molecules**19**(4),4265(2014);https://doi.org/10.3390/molecules19044256
[3] J. Zhang, Y. Han, Langmuir **24**(3), 796 (2008);https://doi.org/10.1021/la702567w
[4] C.Gu, J.Tu, Langmuir**27**(16), 10132 (2011);https://doi.org/10.1021/la200778a
[5] W. Xu, X. Shi, S. Lu, Materials Chemistry and Physics **129**(3), 1042 (2011);https://doi.org/10.1016/j.matchemphys.2011.05.053
[6] K. Liu, X. Yao, L. Jiang, Chemical Society Reviews **39**(8), 3240 (2010);https://doi.org/10.1039/B917112F
[7]A. Garcia-Giron, J. M. Romano, A. Batal, et al, Langmuir**35** (15), 5353 (2019);https://doi.org/10.1021/acs.langmuir.9b00398
[8] J. Li, Y. Zhou, W. Wang, et al, Langmuir**36**(5), 1075 (2020);https://doi.org/10.1021/acs.langmuir.9b02273
[9] J. M. Romano, M. Gulcur, A. Garcia-Giron, et al, Applied Surface Science**476**, 850 (2019);https://doi.org/10.1016/j.apsusc.2019.01.162
[10] V. S. Saji, Advances in Colloid and Interface Science**283**, 102245 (2020);https://doi.org/10.1016/j.cis.2020.102245
[11] H. Yang, Y. Gao, G. S. Frankel, et al, Applied Surface Science**499**, 143916 (2020);https://doi.org/10.1016/j.apsusc.2019.143916
[12] D. Wei, J. Wang, Y. Liu, et al, Chemical Engineering Journal**404**, 12644 (2021);https://doi.org/10.1016/j.cej.2020.126444
[13] S. M. Emarati, M. Mozammel, Ceramics International**46** (2), 1652 (2020);https://doi.org/10.1016/j.ceramint.2019.09.137
[14] H.Khaleghi, A.Eshaghi, Surfaces and Interfaces**20**, 100559

(2020);https://doi.org/10.1016/j.surfin.2020.100559
[15] E. Liu, X. Yin, J. Hu, et al, Colloids and Surfaces A: Physicochemical and Engineering Aspects**586**, 124223 (2020);https://doi.org/10.1016/j.colsurfa.2019.124223
[16] E. Khalili, M. Sarafbidabad, Surfaces and Interfaces**8**, 219 (2017);https://doi.org/10.1016/j.surfin.2017.06.008
[17] Y. L. Qu, M. Zhang, J. Yang, H. D. Yu, Materials Reports **33**(16),2715 (2019);10.11896/cldb.18070134
[18] S. Kim, H. J. Hwang, H. Cho, et al, Chemical Engineering Journal**350**, 225 (2018);https://doi.org/10.1016/j.cej.2018.05.184
[19] H. Cho, J. Chung, G. Shin, et al, Nano energy**56**, 56 (2019);https://doi.org/10.1016/j.nanoen.2018.11.039
[20] T. Liu, Y. Liu, Y. L. Di, H. D. Wang, B. Y. Zheng, Surface Technology **49**(07),112 (2020);10.16490/j.cnki.issn.1001-3660.2020.07.014
[21] C. W. Lin, C. J. Chung, C. M. Chou, et al, Thin Solid Films**620**, 88 (2016);https://doi.org/10.1016/j.tsf.2016.07.087
[22] M. Balordi, A. Cammi, G. S. Magistris, et al, Surface and Coatings Technology**374**, 549 (2019);https://doi.org/10.1016/j.surfcoat.2019.06.001
[23] S. Dong, Z. Wang, L. An, et al,Nanomaterials**10**(8), 1509 (2020);https://doi.org/10.3390/nano10081509
[24] R. Schestatsky, C. P. Zucuni, K. S. Dapieve, et al, Journal of prosthodontic research**64**(1), 12 (2019);https://doi.org/10.1016/j.jpor.2019.05.004
[25] C. Panigrahy, A. Seal, N. K. Mahato, Measurement**147**, 106859 (2019);https://doi.org/10.1016/j.measurement.2019.106859
[26] A. Das, V. Chawla, R. S. Matos, H. D. F.Filho, R. P. Yadav, Ş.Ţălu, S. Kumar, Surface and Coatings Technology421,127420 (2021); https://doi.org/10.1016/j.surfcoat.2021.127420
[27] H. Y. Jiang, M. Liu, H. Y. Qi, A. G. Liang, Y. L. Wang, N. N. Sun, Z. Wu, Chemical Tournal of Chinese Universities **41**(06),1313 (2020);10.7503/cjcu20200050
[28] X. Zhang, Y. Si, J. Mo, et al, Chemical Engineering Journal**313**, 1152 (2017);https://doi.org/10.1016/j.cej.2016.11.014
[29] R. Sun, J. Zhao, Z. Li, et al, Progress in Organic Coatings**133**,77 (2019);https://doi.org/10.1016/j.porgcoat.2019.04.020
[30] G. Wang, Y. Shen, J. Tao, et al, Surface and Coatings Technology**329**, 224 (2017);https://doi.org/10.1016/j.surfcoat.2017.09.055
[31] T. Shi, J. Kong, X. Wang, et al, Applied Surface Science**389**, 335(2016);https://doi.org/10.1016/j.apsusc.2016.07.125
[32] J. Gray-Munro, J. Campbell, Materials Letters**189**, 271 (2017);https://doi.org/10.1016/j.matlet.2016.11.102
[33] B. Qian, Z. Shen, Langmuir**21**(20), 9007(2005);https://doi.org/10.1021/la051308c